Miniaturized Electrochemical Flow Cells

ARTICLE *in* ANALYTICAL CHEMISTRY · MARCH 2003

Impact Factor: 5.64 · DOI: 10.1021/ac025970e · Source: PubMed

6 AUTHORS, INCLUDING:

Stephen Gregory Weber
University of Pittsburgh
233 PUBLICATIONS **3,560** CITATIONS

Published in final edited form as:
Anal Chem. 2003 February 15; 75(4): 1031–1036.

Miniaturized Electrochemical Flow Cells

Eskil Sahlin, **Alexandra ter Halle**, **Kathleen Schaefer**, **Jeffery Horn**, **Matthew Then**, and **Stephen G. Weber***
Department of Chemistry, University of Pittsburgh, Pittsburgh, Pennsylvania 15260

Abstract

Several novel types of miniaturized electrochemical flow cells are described. The flow cells are fabricated in fluorinated ethylene propylene using a novel technique where channels with inner diameters down to 13 μm are integrated with electrodes. The channel is formed by shrinking and simultaneous melting of a heat shrink/melt tubing around a channel template (a tungsten wire) and electrodes followed by removal of the channel template. The technique allows incorporation of different electrode materials of different sizes. The electrode configuration consists of one or two working electrodes inside the channel and a counter electrode located in the channel outlet reservoir. Electrode configurations with different channel and working electrode sizes, different electrode materials including carbon fibers, glassy carbon rods, poly(tetrafluoroethylene)/carbon composite material, and platinum wires, and different arrangements have been assembled. Hydrodynamic voltammograms in dual-electrode (generator–collector) experiments indicate good potential control for cells with 25-μm channels, while there is some *iR* drop in cells with 13-μm channels. Cells prepared with a cylindrical working electrode tangent and perpendicular to a flow channel show a flow rate dependence consistent with thin-layer cell behavior. Electrode areas can be made in the range of 10^{-10}–10^{-8} m^2.

The interest in microscale separation systems such as capillary electrophoresis and capillary liquid chromatography has grown enormously during the last 10 years. However, these systems demand detectors with high mass sensitivity. Several such detection techniques are available including laser-induced fluorescence with confocality or sheath flow cells[1] and electrochemical techniques (e.g., amperometry and conductivity).[2] Many analytes are electroactive without derivatization, and electrochemical detection can therefore be an alternative to the more widely used spectroscopic techniques. However, employing electrochemical detectors for microscale separations typically results in alignment problems. Small microelectrodes (typically 5–30 μm) should be aligned relative to a small channel (typically 10–100 μm wide). Even more problematic is the alignment and configuration of dual working electrode systems with high collection efficiency at the downstream working electrode. One way of circumventing the problem is to integrate the electrodes with the channel.[3–13] Integrated electrodes have been manufactured by sputtering metal electrodes,[3,7–10] photolithography,[4,13] or chemical deposition[5,11] at or near the channel outlet and by attaching conducting tubes directly to the capillary.[6,12]

In this article, a technique is described for manufacturing several novel types of miniaturized electrochemical flow cells consisting of microchannels in fluorinated ethylene propylene (FEP) with integrated electrodes inside the channels. Recently, we have developed a new technique for fabricating different channel structures with inside diameters (i.d.s) down to 13 μm in FEP.[14] Here, we further demonstrate how several different electrode materials of different sizes can be integrated with the channels. In addition, we have characterized the electrochemical

* Corresponding author. E-mail: sweber@imap.pitt.edu..

behavior of these small electrochemical flow cells. Ascorbic acid, potassium ferrocyanide, copper–peptide complexes, and dopamine were used as redox-active analytes.

EXPERIMENTAL SECTION

Materials and Tools

Heat shrink/melt tubing with an i.d. of 0.036 in. was purchased from Small Parts, Inc. (Miami Lakes, FL; Part No. U-SMDT-036) and consisted of an outer layer of poly-(tetrafluoroethylene) (PTFE) and an inner layer of FEP. Tungsten wires (13- and 25-μm i.d.) and platinum wire (25-μm i.d.) were obtained from Goodfellow Corp. (Berwyn, PA). Carbon fibers (30-μm i.d.) were obtained from World Precision Instruments, Inc. (Sarasota, FL), and glassy carbon rods (Sigradur G, 1.0-mm diameter) were obtained from Hochtemperatur-Werkstoffe GmbH (Thierhaupten, Germany). The glassy carbon rods were polished with 0.05-μm alumina powder prior to use. A composite material consisting of 75% poly(tetrafluoroethylene) and 25% carbon (PTFE/C) were obtained from Fluorcarbon (Limhamn, Sweden) and shaped to 1.5-mm diameter rectangular parallelepipeds by cutting the material with a razor blade. The electrode material was held in place during heating with a pair of stainless steel tapered tweezers. The tweezers were kept closed with a clamp. Shrinking and simultaneous melting of the tubing was achieved by heating with a heat gun with a variable temperature range of 210–1100 °F (99–593 °C) and equipped with a reduction nozzle. Fused-silica capillaries (with an i.d. of 50 and 700 μm) were purchased from Polymicro Technologies, Inc. (Phoenix, AZ). Silver-containing epoxy was obtained from Epoxy Technology, Inc. (Billerica, MA).

Instrumentation

Cyclic voltammetry was performed with a model DLK-100A electrochemical analyzer (Analytical Instrument Systems, Inc., Flemington, NJ). Amperometric detection was performed using an Epsilon LC electrochemical detector (Bioanalytical Systems, Inc., West Lafayette, IN). All electrochemical measurements were performed in a Faraday cage, and an Ag/AgCl (3 M NaCl) reference electrode located in the waste reservoir was used as a counter electrode. All potentials stated are with respect to the Ag/AgCl (3 M NaCl) reference electrode. An Ultra-Plus MicroLC System pump (Micro-Tech Scientific, Sunnyvale, CA) or a Waters 510 pump with flow splitting with an injector with a 0.50- or 1.00-μL injection volume (model 3XL, Scientific Systems, Inc., State College, PA) were used for flow injection analysis measurements. If not otherwise stated, a flow rate of 2.0 μL/min was used. In some experiments, data acquisition and storage was controlled by Matlab with locally written software.

Chemicals and Solutions

All chemicals were of analytical grade and all solutions were prepared using MilliQ water from a Millipore system.

The mobile phase for potassium ferrocyanide consisted of 0.20 M carbonate buffer, pH 9.80, and was prepared from sodium bicarbonate and sodium hydroxide. The mobile phase for dopamine consisted of 0.20 M phosphate buffer, pH 7.00, and was prepared from potassium hydrogen phosphate and potassium dihydrogen phosphate. The mobile phase for ascorbic acid was 0.1% trifluoroacetic acid, 3% 1-propanol in water. Conditions for the determination of Cu–peptide complexes are the same as in ref [14].

Fabrication Technique

The manufacturing procedure for the channels with perpendicularly integrated electrodes included the following steps. Holes in the heat shrink/melt tubing for the working electrode(s) were made with a small needle, and the working electrode(s) (glassy carbon rod, carbon fiber, PTFE/C pieces, or platinum wire) was aligned as shown in Figure 1a(1). A tungsten wire was

threaded through a 50-μm-i.d. fused-silica capillary, the heat shrink/melt tubing, and a 700-μm fused-silica capillary (see Figure 1a(1)). The heat shrink/melt tubing was compressed over the electrode(s) with a pair of tweezers so that the working electrode material was pressed against the tungsten wire. The pair of tweezers was kept closed with a clamp. When heated (>350 °C), the outer PTFE layer shrinks and the inner FEP layer melts. Hence, all empty space will be filled with FEP inside the heat shrink/melt tubing. After completion of the shrinking and melting process, the FEP channel/electrode unit was allowed to cool to room temperature while keeping the pair of tweezers closed. During initial cooling, the tungsten wire was pulled back and forth in the channel a few times to prevent it from sticking to the wall. When cooled to room temperature, the pair of tweezers was removed and the FEP device was inspected under a microscope. Contact between the tungsten wire and the working electrode material was confirmed by measuring the electrical conductivity between the tungsten wire and the electrode material followed by removal of the tungsten wire (by pulling it out). The final design is shown in Figure 1b(1). The FEP channel/electrode unit was glued with fast-hardening epoxy glue to a microscope glass slide, and electrical contact with the electrode(s) was achieved by conducting silver-containing epoxy. Curing of the epoxy glue was performed at room temperature. Finally, the exterior was covered with Torr Seal (Varian Vacuum Products, Lexington, MA) in order to protect the electrode. Note that the active electrode surface of an integrated electrode only constitutes the small contact area between the channel and the adjacent electrode material as illustrated in Figure 1c; i.e., the area of the active electrode surface is considerably smaller than the overall area of the electrode material.

The manufacturing procedure for the channels with parallel integrated electrodes consists of the following steps. A 25-μm-diameter tungsten wire was threaded successively through a 50-μm-i.d. silica tubing and a 180-μm-i.d. silica tubing. Under the microscope a 10-μm carbon fiber was threaded in the 50-μm silica tubing. This step determines the length of the working electrode (<100–1650-μm-long electrodes were prepared). A heat shrink/melt tubing was positioned to surround the junctions between the fused-silica capillaries (see Figure 1a(2)). The whole system was slightly pressed between two Pyrex plates. The plates were heated to ~350 °C with a heat gun. The completion of the shrinking and melting process was controlled visually. The system was removed from the plates and allowed to cool to room temperature. The tungsten wire was pulled back and forth as described in the previous procedure and then slowly pulled out after cooling. The device was inspected under the microscope. The length of the carbon fiber in the silica tubing was measured. If the carbon fiber was stuck to the inner wall of the fused-silica tubing, pumping solvent into the device unstuck the carbon fiber from the wall. The length of the carbon fiber in the silica tubing after the shrinking and melting process differs from the initial position of the carbon fiber by ~100 μm. The final design of the device is shown in Figure 1b(2). As in the previous fabrication, the device was glued to a microscope plate. The electrical contact was achieved by gluing the electrode to copper wire with conducting epoxy. The length of the carbon fiber from the FEP tubing to the copper was reduced to a minimum (a few millimeters).

RESULTS AND DISCUSSION

Well over 70 cells have been constructed and tested under different conditions over about 1.5 years. Results shown here are typical. The electrode configurations that were manufactured are given in Table 1. In the two-electrode cells, the distance between the two working electrodes varied between 1.0 and 1.5 mm and the distance between the downstream working electrode and the channel outlet (into the larger fused-silica capillary) varied between 2 and 3 mm. These distances were not rigorously controlled, though there is no reason to expect that to be a challenge. Metal wires, glassy carbon rods, and PTFE/C pieces were always successfully incorporated and functioned well, while the carbon fibers occasionally broke during the shrinking and melting process. Since the electrodes are located within the channels as part of

the channel wall except for configuration F, the contribution to band broadening is extremely small. Furthermore, although the described fabrication technique is not suitable for mass production of flow cells, the technique allows flow cells to be fabricated directly onto the end of many types of capillaries[14] (here this is demonstrated using fused-silica capillaries). Hence, the connection between the electrochemical flow cell and a capillary from, for instance, a capillary liquid chromatography system will have zero dead volume.

Microscopic photographs of 25-μm-diameter channels with two integrated carbon fibers (30-μm diameter, style A) and with two integrated glassy carbon rods (1-mm diameter, style C) are shown in Figure 2a and b, respectively. A photograph of a rigidly held 10-μm carbon fiber (style F) is shown in Figure 3.

The construction procedure does not permit control over the electrode area, nor is the electrode surface particularly easy to see. We therefore estimate the area from a cyclic voltammogram. Assuming that the electrochemical cell behaves as a capacitor, the capacitance per area, *C*, for an electrode can be calculated from a cyclic voltammogram according to[15]

$$C = \Delta i / (2 A v) \quad (1)$$

where Δi is the difference between the anodic and the cathodic current, *A* is the electrode area, and *v* is the scan rate. Using a scan rate of 50 mV/s in 0.20 M sodium carbonate buffer, pH 9.80, 12 new-style A units had an initial Δi at +0.40 V in the range 4–25 pA for 8 of these, and in the range 60–100 pA for 3 of these, and one had initial Δi equal to 400 pA. An exact value of *C* for carbon materials depends on, for example, the material, the polishing procedure, and the potential history of the electrode, but a typical value is in the range 20–70 μF/cm^2.[16] Using *C* equal to 50 μF/cm^2, an electrode with Δi equal to 25 pA can be estimated from eq 1 to have an electrode area of 5×10^{-10} m^2. This area is equal to 25% of the area of a sphere with the same diameter as the channel (25 μm). Hence, most of the carbon fibers were reasonably sealed by FEP with only a small part exposed as electrode surface.

Similarly, in a batch of 10 cells of style F, nine functioned (one 10-μm carbon fiber broke). Apparent areas based on the same procedure were in the range of 2.2×10^{-9}–1.8×10^{-8} m^2. In this set of cells, fiber lengths were purposely varied and made long (eight in the range 700–1650 μm, one at <100 μm). Steady-state current signals (ascorbate, nA/μM) were correlated with the apparent area ($r = 0.94$, $n = 9$) for these cells.

A potential problem with these cells is the inability to polish them. While it is true that we did not challenge the cells severely, with time, as electrodes do, sensitivity was lost. We found that potentiostating the electrodes to +1.50 (or +1.60 V for the 13-μm channels to make up for *IR* loss) for 3 min not only brought the sensitivity to relatively reproducible value but minimized the drift in sensitivity over the short term (hours). Figure 4 shows representative flow injection data of 100 μM potassium ferrocyanide. The top panel shows data from cell configuration C while the lower panel shows data for cell configuration B, made with a composite electrode. The PTFE/C surfaces are inherently more drift free than the glassy carbon, but the anodic treatment works well for it as well. Typically, the cells could be used for at least two weeks with negligible change in the sensitivity.

Electrodes of styles A–D are intended to mimic standard cells, such as the BAS dual-electrode thin-layer cell, which are often used in a series generator–collector configuration.[17] Hydrodynamic voltammograms for 100 μM ferrocyanide using electrode configurations C and D are shown in Figure 5. The upstream anode's potential is changing while the downstream electrode's potential is kept constant at −0.10 V to reduce Fe(III) to Fe(II). There is apparently some *IR* drop shifting the wave position for configuration D with the smaller, 13-μm channel. The collection efficiencies are about 12.5% for style C and 8.0% for style D. These collection

efficiencies are smaller than those recorded for millimeter-sized electrode pairs because of the relatively large spacing between generator and collector.

High collection efficiencies (>80%) have been reported for interdigitated microarray electrodes[18,19] and are a result of short distances (typically in the micrometer range) between the electrodes. The integration of interdigitated microarray electrodes[18,19] into an FEP channel using the methods described here would have some advantages. By integrating such microarray electrodes with the channels, the collection efficiencies will most likely be improved and the distance between the working electrodes will be fixed.

Style F cells are intended to be a more robust replacement for detectors made by inserting a carbon fiber into the effluent from a chromatographic column. Hydrodynamic voltammograms for the biuret complex of tetraglycine with style F cells are well-formed. For style F cells, a comparison can be made to approximately equivalent cells made from a carbon fiber cylinder electrode placed with a micromanipulator into the lumen of a 50-μm capillary. A 400-μm-long fiber placed in the lumen of a fused-silica capillary gives a sensitivity (steady-state current per concentration) of 198 pA/μM (SD 5, $n = 8$) for the biuret complex of the tetrapeptide GGFL and 252 pA/μM (SD 14, $n = 8$) for the biuret complex of the pentapeptide YGGFL at a flow rate of 1.5 μL/min. A style F cell with a fiber length estimated to be 660 μm and operated at 5 μL/min gave a sensitivity of 40 pA/μM (SD 3, $n = 3$) for the biuret complex of the tetrapeptide GGFL and 33 pA/μM (SD 3, $n = 3$) for the biuret complex of the pentapeptide YGGFL. Thus, the sensitivity of the style F electrodes is lower than expected.

The flow rate dependence of the current can lead to an understanding of the geometry of the cell.[20] Figure 6 shows, over a wide flow rate range (in μL/min), for style C (bottom) and style D (top) a linear relationship between log(coulometric yield) and log(flow rate) with slopes of −0.66 (bottom, C) and −0.61 (top, D) consistent with thin-layer cell behavior.[20] It is interesting to note that the fluid velocities at the highest flow rates used were 6.3 and 3.4 m/s for the 13- and 25-μm channels, respectively. The electrodes are separated on the order of 1 mm, so the travel time between the up- and downstream electrodes is in the 1-ms range.

Detection limit for ferrocyanide was estimated to be 88 nM (based on three times the standard deviation of the blank injection in flow injection analysis). Clearly this is a conservative estimate for chromatographic applications where the noise arises from an electronic and environmental source rather than injection transients. A calibration curve for ferrocyanide is linear from 500 nM to at least 100 μM.

A hydrodynamic voltammogram for dopamine (10 μM) in 0.20 M phosphate buffer, pH 7.00, using a 25-μm-diameter channel and a 30-μm-diameter carbon fiber (upstream electrode at cell configuration A) is shown in Figure 7. Also shown are the response at +0.60 V and a corresponding blank. The noise (standard deviation) of the blank over the period from 1 to 2 min is under 40 fA. The calculated detection limit (S/N = 3) is on the order of 15 nM. This is in the same range as for millimeter-dimensioned systems.

The cells described here have all been used numerous times, under pressures as high as 10 atm or more. They are chemically inert except to very strong reducing agents. While certainly the “handmade” aspect of the technique makes it inapplicable to problems more suited to “chips”, the chemical inertness and ruggedness suggest applicability in routine laboratory and plant measurement situations. Facile integration with capillary devices allows zero dead volume connections. The detection limits with these detectors (e.g., Figure 7) are superior (by 40 times) to microfabricated systems which are in the 0.5–1 μM range.[21,22]

Acknowledgements

We acknowledge NIH for financial support through Grants GM 44842 and DA 14926, P.T. Kissinger at Bioanalytical Systems, Inc. for providing the Epsilon LC electrochemical detector, and Amy Beisler for technical assistance.

References

1. Tao L, Kennedy RT. TrAC, Trends Anal Chem 1998;17:484–491.
2. Wang AB, Fang YZ. Electrophoresis 2000;21:1281–1290. [PubMed: 10826671]
3. Voegel PD, Zhou WH, Baldwin RP. Anal Chem 1997;69:951–957.
4. Woolley AT, Lao KQ, Glazer AN, Mathies RA. Anal Chem 1998;70:684–688. [PubMed: 9491753]
5. Li T, Coufal P, Opekar F, Stulik K, Wang E. Anal Chim Acta 1998;360:53–59.
6. Zhong M, Lunte SM. Anal Commun 1998;35:209–212.
7. Voegel PD, Baldwin RP. Electrophoresis 1998;19:2226–2232. [PubMed: 9761208]
8. Chen DC, Chang SS, Chen CH. Anal Chem 1999;71:3200–3205.
9. Wang J, Tian BM, Sahlin E. Anal Chem 1999;71:3901–3904.
10. Martin RS, Gawron AJ, Lunte SM, Henry CS. Anal Chem 2000;72:3196–3202. [PubMed: 10939387]
11. Hilmi A, Luong JHT. Anal Chem 2000;72:4677–4682. [PubMed: 11028630]
12. Hua L, Tan SN. Anal Chem 2000;72:4821–4825. [PubMed: 11055695]
13. Gavin PF, Ewing AG. Anal Chem 1997;69:3838–3845.
14. Sahlin E, Beisler AT, Woltman SJ, Weber SG. Anal Chem 2002;74:4566–4569. [PubMed: 12236370]
15. Bard, A. J.; Faulkner, L. R. In Electrochemical Methods, Fundamentals and Applications, 2nd ed.; John Wiley & Sons: New York, 2001; pp 11–18.
16. McCreery, R. L.; Cline, K. K. In Laboratory Techniques in Electroanalytical Chemistry, 2nd ed.; Kissinger, P. T., Heineman, W. R., Eds.; Marcel Dekker: New York, 1996; pp 293–332.
17. Roston DA, Kissinger PT. Anal Chem 1982;54:429–434.
18. Bjorefors F, Strandman C, Nyholm L. Electroanalysis 2000;12:255–261.
19. Kurita R, Tabei H, Liu ZM, Horiuchi T, Niwa O. Sens Actuators, B 2000;71:82–89.
20. Weber SG. J Electroanal Chem 1983;145:1–7.
21. Manica DP, Ewing AG. Electrophoresis 2002;23:3735–3743. [PubMed: 12432536]
22. Wang J. Talanta 2002;56:223–231.

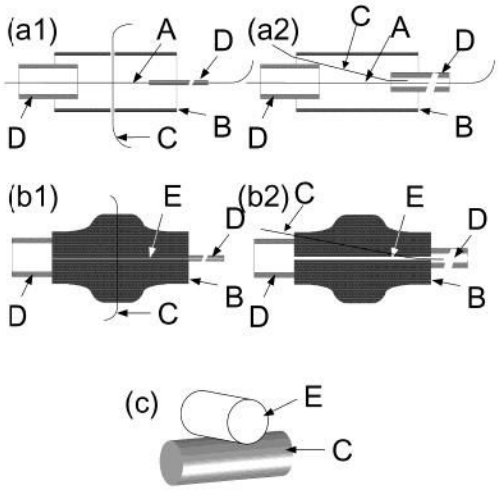

Figure 1.

Schematic drawing of (a1) alignment of the channel and electrode prior to heating for styles A–E, (a2) for style F; (b1) final design for styles A–E and (b2) for style F; and (c) alignment of the channel relative to the electrode for styles A–E. (A) Tungsten wire, (B) heat shrink/melt tubing, (C) working electrode material (carbon fiber, glassy carbon rod, PTFE/C piece, or metal wire), (D) fused-silica capillary, and (E) channel. Objects in the figure are not drawn to scale for clarity.

Figure 2.
Microscopic photographs of 25-μm-diameter channels with integrated electrodes. (a) Channel with two 30-μm-diameter carbon fibers and (b) channel with two 1.0-mm-diameter glassy carbon rods.

Figure 3.
Microscopic photograph of a 50-μm fused silica containing a 10-μm-diameter carbon fiber and leading into a 25-μm channel in FEP.

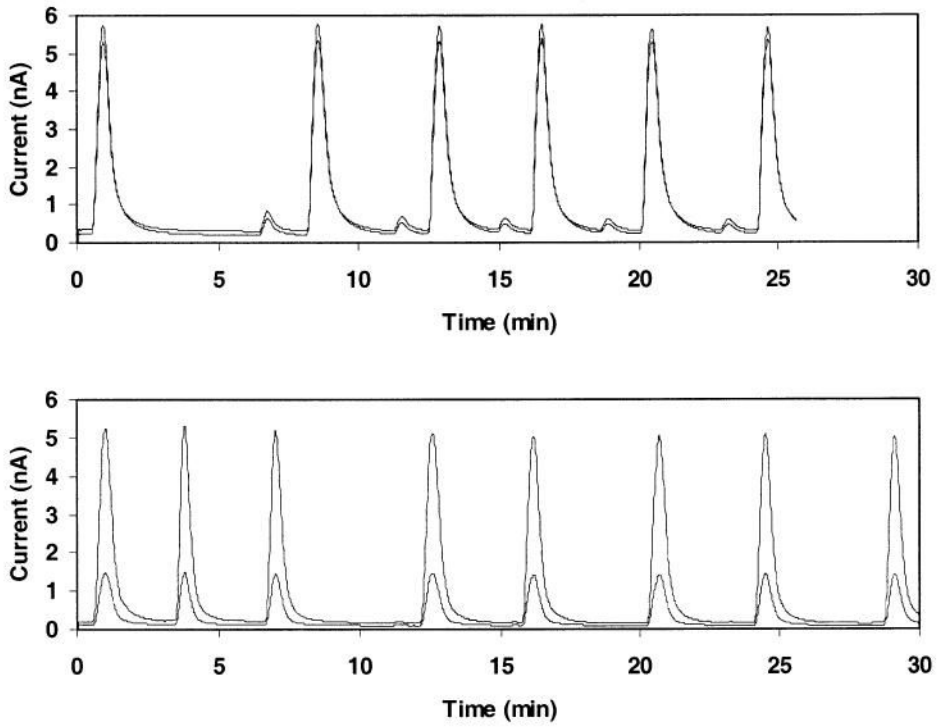

Figure 4.

Flow injection (0.50-μL injection volume) of 100 μM potassium ferrocyanide repeatedly in 0.20 M carbonate buffer, pH 9.80, at a flow rate of 2.0 μL/min. Top panel: cell configuration C (upstream and downstream electrode). Bottom panel: cell configuration B, upstream (smaller signals) and downstream (larger signals) electrode. Detection at +0.90 V at all electrodes.

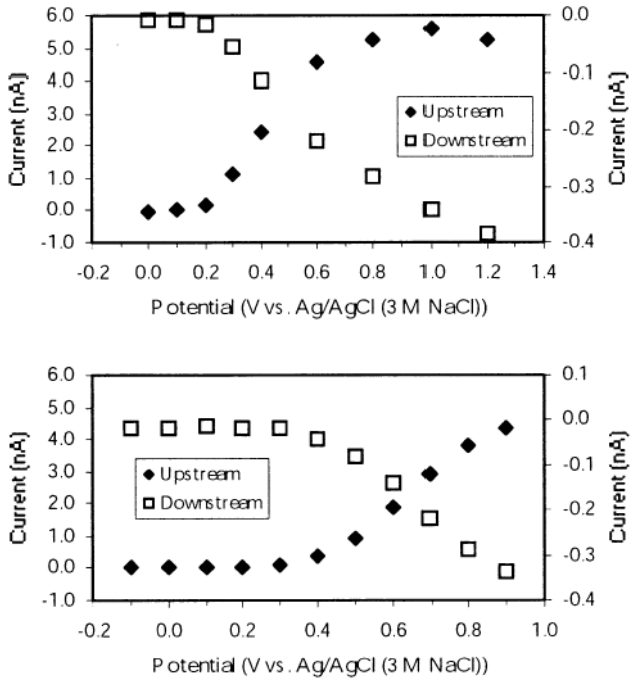

Figure 5.

Hydrodynamic voltammograms for 100 μM potassium ferrocyanide, styles C (top) and D (bottom). The white squares are the downstream collector and have the right scale; the black symbols are the upstream generator and have the left scale. The downsteam electrode is kept at −0.10 V while the potential at the upstream electrode is changed. Measurements were performed in 0.20 M carbonate buffer, pH 9.80, at a flow rate of 2.0 μL/min using an injection volume of 0.50 μL.

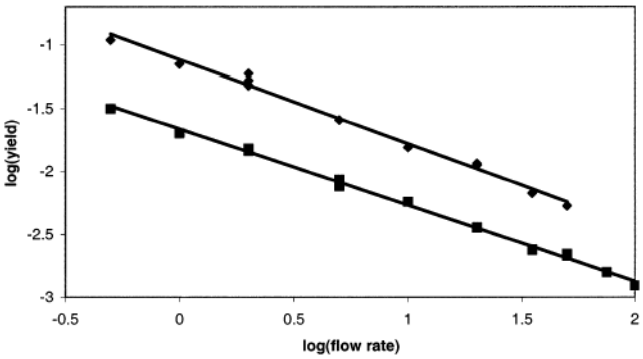

Figure 6.
Working electrode coulometric efficiency for 100 μM potassium ferrocyanide as a function of flow rate (μL/min) for electrode configurations C (bottom) and D (top). Measurements were performed in 0.20 M carbonate buffer, pH 9.80, using an injection volume of 0.50 μL and detection at +0.80 V.

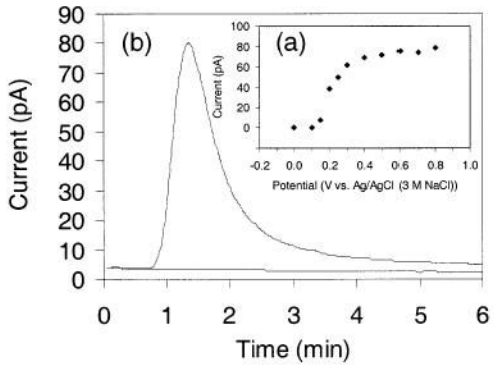

Figure 7.

(a) Hydrodynamic voltammogram for 10 μM dopamine in 0.20 M phosphate buffer, pH 7.00. (b) Signal obtained at +0.60 V and a corresponding blank. Measurements were performed using a 25-μm-i.d. channel and a 30-μm-diameter carbon fiber at a flow rate of 2.0 μL/min and an injection volume of 0.50 μL.

Table 1

Fabricated Channels and Electrode Configurations[a]

configuration	channel diam (μm)	working electrode(s)
A	25	two 30-μm-diameter carbon fibers[b]
B	25	two 1.5-mm-diameter PTFE/C rectangular parallelepipeds[b]
C	25	two 1-mm-diameter glassy carbon rods[b]
D	13	two 1-mm-diameter glassy carbon rods[b]
E	25	one 25-μm-diameter platinum wire[b]
F	25	one 1-μm-diameter carbon fiber[c]

[a] All configurations included an outlet reservoir.

[b] Electrodes perpendicular to flow axis.

[c] Electrode parallel to flow axis.